Published in final edited form as:
Integr Biol (Camb). 2013 November ; 5(11): 1385–1392. doi:10.1039/c3ib40121a.

Bioactive sphingolipid metabolites modulate ovarian cancer cell structural mechanics

Hesam Babahosseini[a,d], **Paul C. Roberts**[b], **Eva M. Schmelz**[c], and **Masoud Agah**[d]

Hesam Babahosseini: hbabahosseini@vt.edu; Paul C. Roberts: robec06@vt.edu; Eva M. Schmelz: eschmelz@vt.edu; Masoud Agah: agah@vt.edu

[a]Department of Mechanical Engineering, 100 Randolph Hall, Blacksburg, VA, USA. Fax: +1-540-231-3362; Tel: +1-540-231-4180

[b]Department of Biomedical Sciences and Pathobiology, Virginia-Maryland Regional College of Veterinary Medicine, Corporate Research Center, Building 23 (ILSB), 1981 Kraft Drive (0913), Blacksburg, VA 24061, USA. Fax: +1-540-231-3414; Tel: +1-540-231-7949

[c]Department of Human Nutrition, Foods and Exercise, Corporate Research Center, Building 23 (ILSB) 1981 Kraft Drive, Blacksburg, VA 24061, USA. Fax: +1-540-231-5522; Tel: +1-540-231-3649

[d]VT MEMS Laboratory, The Bradley Department of Electrical and Computer Engineering, 469 Whittemore Hall, Blacksburg, VA 24061, USA. Fax: +1-540-231-3362; Tel: +1-540-231-2653

Abstract

Cancer progression is associated with an increased deformability of cancer cells and reduced resistance to mechanical forces, enabling motility and invasion. This is important for metastases survival and outgrowth and as such could be a target for chemopreventive strategies. In this study, we determined the differential effects of exogenous sphingolipid metabolites on the elastic modulus of mouse ovarian surface epithelial cells as they transition to cancer. Treatment with ceramide or sphingosine-1-phosphate in non-toxic concentrations decreased the average elastic modulus by 21% ($p \leq 0.001$) in transitional and 15% ($p \leq 0.02$) in aggressive stages while exerting no appreciable effect on non-malignant cells. In contrast, sphingosine treatment on average increased the elastic modulus by 33% ($p \leq 0.0002$) in aggressive cells while not affecting precursor cells. These results indicate that tumor-supporting sphingolipid metabolites act by making cells softer, while the anti-cancer metabolite sphingosine partially reverses the decreased elasticity associated with cancer progression. Thus, sphingosine may be a valid alternative to conventional chemotherapeutics in ovarian cancer prevention or treatment.

Introduction

During the progression of cancer, cells undergo numerous genetic and epigenetic changes that impact critical functions such as growth, motility, metabolism, communication, and others.[1] In addition, alterations of the cells' mechanical phenotype, including changes in cell structure, morphology, and responses to mechanical stimuli, have been reported to accompany cancer progression.[2] These result in an increased deformability of malignant cells and an enhanced migration capability–both effects are directly correlated with increased malignancy and metastasis.[3] Therefore, the structural and mechanical properties of cells could be exploited for effective characterization of cancer cells. Several experimental techniques including micropipette aspiration,[4] optical tweezers,[5] optical stretching

Correspondence to: Eva M. Schmelz, eschmelz@vt.edu; Masoud Agah, agah@vt.edu.

rheometry,[6] microplate stretching,[7] magnetic twisting,[8] and most notably atomic force microscopy[9] (AFM) have already been utilized to quantify cell deformation characteristics and to correlate them with cancer progression. AFM is a well-established tool for mechanical characterization of biological cells under physiological conditions at a single cell level. This microscopy technique has been used to confirm the differences in cellular stiffness of benign and malignant bladder,[10] prostate,[11] lung,[12] blood,[13] and breast[14] epithelial cells. AFM has also been used to evaluate the effect of anti-cancer drugs providing insights into the sensitivity and efficiency of chemotherapies via biomechanical profiling of cells in response to treatment.[15] In this regard, it has been reported that upon short-term treatment with anti-cancer drug doxorubicin, both elastic modulus and adhesion force of human lung adenocarcinoma cells, measured quantitatively by AFM, were found to be increased while those of non-transformed human epithelial cells were decreased.[16] Moreover, results of two separate studies revealed that EGCG, a known potential anti-cancer polyphenol in green tea [17] can cause a significant increase in stiffness of metastatic tumor mesothelial[18] and melanoma[19] cells. In another study via AFM, dexamethasone or daunorubicin chemotherapy increased leukemia cells' stiffness.[20] Recently, Sharma et al. have also found that the softening trend of ovarian cancer cells in the process of malignancy was reversed after cisplatin treatment.[21] The dose-dependent rate of stiffening was affected by the remodeling of the F-actin polymerization.[21] These studies suggest that cell stiffness measured by AFM can be used as a potential biomarker to predict the progression of cancer, its metastatic potential, and its response to drug treatment. In our previous studies,[22] we have employed AFM to determine changes in the mechanical responses during ovarian cancer progression. For these studies, we utilized our mouse ovarian surface epithelial (MOSE) cell system, a syngeneic model for progressive ovarian cancer that represents early/benign, intermediate/transitional, and late/malignant stages of ovarian cancer.[23] As MOSE cells progress, they exhibit alterations in their phenotype: they become smaller and their cytoskeleton becomes increasingly disorganized, with significant losses in filamentous actin.[24] This is associated with increasing softness and decreased viscosity[22a], determined by the actin cytoskeleton organization.[22b] Since the cytoskeleton determines not only the shape and structural integrity of cells but connects the extracellular physical, physiological and biochemical environment and the cell surface to intracellular signaling pathways and gene transcription,[25] it plays a distinct role in the regulation of cell growth, motility, senescence, and apoptosis.[25a, 26]

The bioactive sphingolipid metabolites ceramide (Cer), sphingosine (So), and sphingosine-1-phosphate (S1P) play significant roles in the cells' response to intra- and extracellular stimuli; as lipid second messengers, they regulate cell growth, death, motility, and many more cellular functions and processes.[27] So and Cer are generally pro-apoptotic and anti-proliferative[27a] and have been shown to inhibit growth and induce apoptosis in cancer cells.[28] However, Cer also increases inflammation and therefore exerts a pro-tumorigenic effect.[29] In contrast, S1P often induces cell growth, survival, motility, angiogenesis and thereby can support tumor development.[30] These second messengers are rapidly inter-convertible and the sphingolipid profile generated in a cell will determine how the cells respond to the stimulus. Hence, the effect is typically context dependent and impacted by the cells origin, its function, and environment (among other variables). We have previously shown that complex sphingolipids administered orally suppress colon[28, 31] and breast cancer progression.[32] The regulation of cell growth rather than overt toxicity towards transformed cells seems to be one of the underlying mechanisms of tumor suppression by sphingolipids.[31a, 31b] Sphingolipid metabolites also differentially modulate the cellular architecture and the cytoskeleton organization in various cell lines.[33] However, the impact of sphingolipid treatment on the biomechanical properties of ovarian cancer cells representing different stages of aggressiveness is not known. Here we determined if these bioactive metabolites can reverse the aberrant biomechanical properties and responses of

aggressive cancer cells, shifting them towards their benign precursor counterparts. Our results demonstrate that the biomechanics of aggressive cancer cells are modulated by sphingolipids and that exogenous So treatment may offer the means to deter tumor growth and metastasis by reversing aberrant biomechanical properties.

Experimental methodology

Cell Culture and Sample Preparation

The MOSE cell lines were generated from mouse ovarian surface epithelium as described.[23] The cells are categorized into early (passage no. 15-25) (MOSE-E), intermediate (passage no. 75-80) (MOSE-I), and late stage (passage no. 155-171) (MOSE-L) based on their phenotype. During progression, changes in the genotype include genes encoding cytoskeleton proteins and their regulators.[24] The cells were routinely grown in High Glucose Dulbecco's Modified Eagle's Medium (Sigma Aldrich), containing 4% fetal bovine serum (Atlanta Biological), 3.7 g/L of sodium bicarbonate, and 1% penicillin/streptomycin (Sigma Aldrich). To mimic the exposure to sphingolipid metabolites over time in a prevention regimen, the cells were grown in non-toxic concentrations of So (1.5 μM) (Avanti Polar Lipids) for at least three passages. To investigate the impact of potentially pro-tumorigenic metabolites, cells were also treated with Cer (2 μM), and S1P (500 nM). For AFM determinations, the cells were seeded at 1×10^5 cells per 12 mm^2 glass coverslips coated with 0.1 mg/mL collagen type IV (Sigma) for 24-30 hrs prior to the AFM experiments to allow the cells to attach. The measurements were carried out on single cells in their respective culture medium at room temperature. A buffered HEPES solution was added to the coverslip samples (final concentration of 13.5 mM) to maintain a physiological pH of 7.2 during about 2-3 hrs test sessions.

Atomic Force Microscopy

Measurements were performed via a Multimode V SPM atomic force microscope (Veeco Instruments, Santa Barbara, CA) in integration with an inverted optical microscope. Soft V-shaped SiNi cantilevers, TR400PSA (Olympus, Tokyo, Japan), with an approximate length of 200 μm and a nominal spring constant of 0.02 N/m were used for the indentation of adherent cells (Fig. 1). The practical spring constant of the cantilevers was experimentally measured using thermal noise fluctuation. A glass microsphere bead (Duke Scientific, Palo Alto, CA) with an approximate diameter of 10 μm was attached to the sharp cantilever tip using a two-part epoxy (Miller Stephenson, Sylmar, CA) to increase the total surface contact area and as a consequence reduce the indentation stress on the soft biological samples and remove any nonlinearity in deformation. The exact size and the location of the attached glass bead on the cantilever were identified via a HIROX KH-7700 3D Digital Video Microscope. Since the elastic modulus of cells depends on the indentation location and speed,[34] the indentations were performed at the cells' nuclei region and at an approach velocity of ∼0.5 μm/s. Cantilever deflection vs. piezo displacement data were acquired at a sample rate of 5 kHz. To keep the validation of applying the Hertz model to the data, the indentation depth was kept up to 30% of total sample height by limiting the maximum indentation force to a trigger of 1.5±0.3 nN.[35]

Data Analysis

AFM is a powerful tool, capable of obtaining cantilever force vs. piezo displacement via indentations at the nanoscale (Fig. 2). The cantilever deflection is sensed using an optical method in AFM. For a negligible cantilever deflection in comparison to the cantilever length, the cantilever force-*F* is linearly proportional to the cantilever deflection-*d* by the spring constant of the cantilever-*k*. The force curve should be converted to the force vs. tip-sample separation distance curve in order to estimate the sample's elastic modulus. The tip-

sample separation distance-*D* is described as the difference of the piezo position-*z* and the cantilever deflection-*d*. Elastic modulus of the sample can be calculated by fitting a proper contact model theory to the (*F*, *D*) curve. Several continuum contact mechanics models such as DMT, JKR, and Hertz models have been developed to describe the micro-scale deformations. The Sneddon's extended version of the Hertz model is a simple and applicable theory for soft materials like biological cells which is used here.[36] The model correlates the applied force-*F* and the induced indentation depth-δ in interaction between a spherical object and a sample as follow:

$$F=\frac{4}{3}E^{*}\sqrt{R}.\delta^{\frac{3}{2}} \quad (1)$$

where *R* is the radius of the spherical glass bead attached on the cantilever and *E** is relative elastic modulus of contact surfaces. For the infinitely hard tip $E_{\text{tip}} \gg E_{\text{cell}}$, the relative elastic modulus is $E^{*}=E_{cell}/(1-\nu_{cell}^{2})$, where E_{cell} is elastic modulus and ν is Poisson's ratio of the cell. Cells' Poisson's ratio is assumed to be 0.5 for incompressible biological cells.[37] The indentation depth is described as the difference in the relative movement of the piezo scanner-z and the cantilever deflection-d as the following:

$$\delta=(z-z_{0})-(d-d_{0}) \quad (2)$$

where z_0 and d_0 are the piezo scanner position and the cantilever deflection at the initial contact point of the probe with the cell. It is easier to find the elastic modulus and the initial contact point using a linear version of the Hertz's model eqn (1) in respect to the deformation-δ[38] as the following form:

$$F^{\frac{2}{3}}=\left[\frac{4\sqrt{R}}{3\left(1-\nu_{cell}^{2}\right)}E_{cell}\right]^{\frac{2}{3}}(z-d)-\left[\frac{4\sqrt{R}}{3\left(1-\nu_{cell}^{2}\right)}E_{cell}\right]^{\frac{2}{3}}(z_{0}-d_{0}) \quad (3)$$

All the data analysis was implemented via MATLAB 2010a software.

Results

The AFM experiments were conducted on both control and sphingolipid-treated MOSE cells to obtain cantilever force vs. piezoelectric displacement via indentation as schematically shown in Fig. 2. The Hertz model fitted well to the acquired experimental data from 40-70 single cells randomly selected from each cell line/drug treated population with a high correlation coefficient ($0.85 \leq R^2 \leq 0.99$) to obtain their elastic modulus. To minimize the effects of external and random variances in the experimental results as well as validate reproducibility of them, at least three separate AFM tests were conducted for each cell population. Within the same cell population, there was not more than 5% variation between the measured average elastic moduli of two AFM tests.

The population histograms generated by combining all measured elastic modulus responses from control and So, Cer, and S1P treated MOSE cells representing late, intermediate, and early stages of cancer progression are depicted in Fig. 2. The average ± standard deviation, and the peak (mode) values (correspond to peak points of Gaussian curves fitted to the elastic moduli distributions) of the measured elastic moduli are also summarized in Fig. 3.

Moreover, the combination of all measured elastic modulus responses for each population are shown in Fig. 4 and compared within each stage of cancer along with the statistical significance of changes (*p*-value) in comparison to the controls. Two sample independent t-tests were used to analyze the statistical significances of the changes in the elastic modulus.

The AFM measurements from early, intermediate, and late stage of untreated MOSE cells show that the average elastic modulus decreased as the cells progressed from a benign to a late, malignant stage, confirming our previous results.[22a] Treatment of MOSE cells with non-toxic concentrations of Cer and S1P showed comparable decreases in the average and the mode elastic modulus values in all three stages compared to their respective control cells.

The average elastic modulus decreased by 13% ($p \approx 0.1$) in MOSE-E, 21% ($p \approx 0.001$) in MOSE-I, and 15% ($p \approx 0.02$) in MOSE-L cells for both Cer and S1P treatment. On the other hand, So treatment resulted in a significant increase in the average and the mode elastic modulus values of the aggressive MOSE-L cells by 33% and 30% ($p \approx 0.0002$), respectively.

MOSE-I cells did not appreciably respond to the So treatment ($p \approx 0.4$) while MOSE-E showed a slight decrease in the average elasticity after So treatment, indicating the cells became softer; however, this was not statistically significant ($p \approx 0.2$).

Together, the results indicate that So treatment can at least partially reverse the decreasing elasticity of aggressive MOSE cells while both Cer and S1P treatment make the cells even softer. Neither treatment significantly impacted the non-malignant MOSE-E cells, suggesting that the treatment with exogenous sphingolipids may not increase the tumorigenic or metastatic properties of non-transformed cells.

Notably, the distributions of the untreated MOSE cells' elastic moduli reshape from a wide distribution for benign/early cells to a sharp concentration for malignant/late cells (Fig. 3A, 3A′, and 3A″). This confirms our previous observations that benign MOSE-E cells are heterogeneous in their biomechanical phenotype but become more homogenous during progression.[22a]

Cer and S1P do not impact the histogram of MOSE-E cells (Fig. 3B and 3C) while they have the same effect on the histograms of MOSE-I, slightly shifting them toward lower stiffness and making the curve slightly sharper (Fig. 3B′ and 3C′). So treatment of MOSE-E or MOSE-I cells also did not affect the distribution of the elastic modulus responses (Fig. 3D and 3D′). This further delineates the lack of impact of the treatments on non-malignant MOSE-E cells. On the other hand, histograms of Cer and S1P treated MOSE-L cells (Fig. 3B″ and 3C″) show a shift toward lower stiffness and a more homogeneous population as indicated by the sharp curves in control MOSE-L. In contrast, So treatment effectively impacted the histogram of MOSE-L cells and notably shifted more cells towards the stiffer values, resulting in a broader distribution curve (Fig. 3D″). However, not all cells responded to the treatment with increased stiffness. The effects of the treatments on the histograms of MOSE-E, MOSE-I, and MOSE-L are depicted and compared in Fig. 3E, 3E′, and 3E″, respectively.

Discussion and Conclusions

In this study, the AFM cell indentation was used as a technique for drug efficacy studies and development. Our findings indicate that non-toxic concentrations of So, a potential tumor suppressing sphingolipid metabolite, can induce aggressive ovarian cancer cells to mechanically behave more like benign cells by rendering them stiffer. Based on our

previous studies, the changes in a cells' elastic modulus response is likely due to the remodeling of the actin cytoskeleton. MOSE-E cells exhibit a well-organized actin cytoskeleton and higher f-actin concentrations while MOSE-L cells exhibit thin and disorganized stress fibers.[23-24] The disruption of the intact actin cytoskeleton in MOSE-E or stabilization in MOSE-L significantly reversed the cells' elastic modulus,[22b] highlighting the importance of the actin cytoskeleton for the biomechanical responses. However, treatment with So improved the actin organization and increased the f-actin levels which was associated with a decrease in invasive capacity;[39] this correlates well with the increase in elastic modulus determined in this study. Conversely, the sphingolipid metabolites associated with supporting cancer growth (S1P) and tumor-promoting inflammation (Cer) decreased the elastic modulus of MOSE cells and made the cells softer; neither Cer nor S1P induced actin stress fiber formation in MOSE-L cells.[39] This is in contrast to the effect in endothelial cells where S1P increases barrier function and peripheral stress fiber organization.[40] The latter may be dependent upon the differentiation and activation status of cells; MOSE-L cells represent a poorly differentiated cell that has clearly undergone an epithelial-to-mesenchymal transition (EMT) phase.[23] Alternatively, responsiveness to S1P may be receptor specific; endothelial cells are known to express predominately S1PR1 and S1PR3. The S1P receptor profile of our MOSE cell lines has not been determined, but they may lack specific S1PR expression or other critical downstream effectors.

Overall, softening and increasing deformability are associated with enhanced capability for metastasis and tissue invasion.[3] Importantly, So treatment of benign MOSE cells did not alter the biomechanical properties of the cells. Future *in vivo* studies will shed light on whether treatments with Cer and S1P lead to an increased transformation and progression of benign and less aggressive ovarian cancer cells. This is especially important since the increased S1P levels in ascites fluid may promote not only the survival of the exfoliated cancer cells and increase adhesion and tumor outgrowth but also could impact the benign ovarian surface epithelial cells.

In summary, extended treatment with non-toxic concentrations of exogenous So partially reversed the aberrant biomechanical properties of aggressive ovarian cancer cells. This is comparable to treatment with conventional chemotherapeutics such as cisplatin but without their deleterious side effects. Thus, future studies will explore if the administration of So can suppress ovarian cancer progression and metastasis and if the biomechanical signature can be used as measure for treatment efficacy.

Acknowledgments

The research is supported by the NSF ECCS-0925945 (to MA), and the NIH R01 CA118846 (to EMS and PCR). The authors would like to thank the Nanoscale Fabrication and Characterization Laboratory (NCFL) at Virginia Tech for equipment support.

Notes and references

1. (a) Alberts, B.; Johnson, A.; Lewis, J.; Raff, M.; Roberts, K.; Walter, P. Molecular biology of the cell. Garland Science; New York: 2002. (b) Ben-Ze'ev A. Cell-Cell Interaction and Cell Configuration Related Control of Cytokeratins and Vimentin Expression in Epithelial Cells and in Fibroblasts. Annals of the New York Academy of Sciences. 1985; 455:597–613. [PubMed: 2417531]
2. (a) Kumar S, Weaver VM. Mechanics, malignancy, and metastatis: The force journey of a tumor cell. J Cancer Metastatis Rev. 2009; 28:113–27.(b) Rao K, Cohen H. Actin Cytoskeletal network in aging and cancer. Journal of Mutation Research. 1991; 256:139–148.
3. Suresh S. Biomechanics and biophysics of cancer cells. Acta Biomater. 2007:413–438. [PubMed: 17540628]

4. Guo Q, Park S, Ma H. Microfluidic micropipette aspiration for measuring the deformability of single cells. Lab Chip. 2012; 12:2687–95. [PubMed: 22622288]

5. Dao M, Lim CT, Suresh S. Mechanics of the human red blood cell deformed by optical tweezers. Journal of the Mechanics and physics of solids. 2003; 51:2259–2280.

6. (a) Guck J, Schinkinger S, Lincoln B, Wottawah F, Ebert S, Romeyke M, Lenz D, Erickson HM, Ananthakrishnan R, Mitchell D, Käs J, Ulvick S, Bilby C. Optical deformability as an inherent cell marker for testing malignant transformation and metastatic competence. Biophysics J. 2005; 88:3689–98.(b) Remmerbach TW, Wottawah F, Dietrich J, Lincoln B, Wittekind C, Guck J. Oral cancer diagnosis by mechanical phenotyping. Cancer Research. 2009; 69:1728–1732. [PubMed: 19223529]

7. Thoumine O, Ott A. Time scale dependent viscoelastic and contractile regimes in fibroblasts probed by microplate manipulation. Journal of Cell Science. 1997; 110:2109–16. [PubMed: 9378761]

8. Swaminathan V, Mythreye K, O'Brien ET, Berchuck A, Blobe GC, Superfine R. Mechanical stiffness grades metastatic potential in patient tumor cells and in cancer cell lines. Cancer Research. 2011; 71:5075–80. [PubMed: 21642375]

9. (a) Lekkaa M, Pogodaa K, Gosteka J, Klymenkoa O, Prauzner-Bechcickia S, Wiltowska-Zubera J, Jaczewska J, Lekki J, Stachura Z. Cancer cell recognition – Mechanical phenotype. 2012; 43:1259–66.(b) Darling EM, Topel M, Zauscher S, Vail TP, Guilak F. Viscoelastic properties of human mesenchymally-derived stem cells and primary osteoblasts, chondrocytes, and adipocytes. Journal of Biomechanics. 2008; 41:454–464. [PubMed: 17825308] (c) Cross SE, Jin Y, Rao J, Gimzewski JK. Applicability of AFM in cancer detection. Nat Nanotechnol. 2009; 4:72–3. [PubMed: 19197298]

10. Lekka M, Laidler P, Gil D, Lekki J, Stachura Z, Hrynkiewicz AZ. Elasticity of normal and cancerous human bladder cells studied by scanning force microscopy. Biophysics J. 1999; 28:312–316.

11. Faria EC, Ma N, Gazi E, Gardner P, Brown M, Clarke NW, Snook RD. Measurement of elastic properties of prostate cancer cells using AFM. Analyst. 2008; 133:1498–1500. [PubMed: 18936825]

12. Cross SE, Jin YS, Rao J, Gimzewski JK. Nanomechanical analysis of cells from cancer patients. Nature Nanotechnology. 2007; 2:780–783.

13. Rosenbluth MJ, Lam WA, Fletcher DA. Force Microscopy of nonadherent cells: A comparison of Leukemia cell deformability. Biophysics J. 2006; 90:2994–3003.

14. (a) Nikkhah M, Strobl JS, Schmelz EM, Agah M. Evaluation of the influence of growth medium composition on cell elasticity. J of Biomechanics. 2011; 44:762–766.(b) Nikkhah M, Strobel JS, De Vita R, Agah M. The cytoskeletal organization of breast carcinoma and fibroblast cells inside three dimensional isotropic silicon microstructures. Biomater. 2010; 31:4552–61.

15. Wanga J, Wan Z, Liu W, Li L, Ren L, Wang X, Sun P, Ren L, Zhao H, Tu Q, Zhang Z, Song N, Zhang L. Atomic force microscope study of tumor cell membranes following treatment with anti-cancer drugs. Biosensors and Bioelectronics. 2009; 25:721–727. [PubMed: 19734031]

16. Xiao L, Tang M, Li Q, Zhou A. Non-invasive detection of biomechanical and biochemical responses of human lung cells to short time chemotherapy exposure using AFM and confocal Raman spectroscopy. Analytical Methods. 2012; 5:874–879.

17. Yang CS, Wang X. Green tea and cancer prevention. Nutrition and Cancer. 2010; 62:931–7. [PubMed: 20924968]

18. Cross SE, Jin YS, Lu QY, Rao J, Gimzewski JK. Green tea extract selectively targets nanomechanics of live metastatic cancer cells. Nanotechnology. 2011; 22:215101. 9pp. [PubMed: 21451222]

19. Suganuma M, Watanabe T, Takahashi A, Fujiki H. Metastatic potential of B16 melanoma subclones indicated by cell stiffness measured by atomic force microscopy (AFM). Cancer Research. 2011; 71(1)

20. Lam WA, Rosenbluth MJ, Fletcher DA. Chemotherapy exposure increases leukemia cell stiffness. Blood. 2006; 109:3505–8. [PubMed: 17179225]

21. Sharma S, Santiskulvong C, Bentolila LA, Rao J, Dorigo O, Gimzewski JK. Correlative nanomechanical profiling with super-resolution F-actin imaging reveals novel insights into

mechanisms of cisplatin resistance in ovarian cancer cells. Nanomedicine. 2012; 8:757–766. [PubMed: 22024198]

22. (a) Ketene AN, Schmelz EM, Roberts PC, Agah M. The effects of cancer progression on the viscoelasticity of ovarian cell cytoskeleton structures. Nanomedicine: nanotechnology, biology, and medicine. 2011; 8:93–102.(b) Ketene AN, Roberts PC, Shea AA, Schmelz EM, Agah M. Actin filaments play a primary role for structural integrity and viscoelastic response in cells. Integrative Biology. 2012; 4:540–549. [PubMed: 22446682]
23. Roberts PC, Mottillo EP, Baxa AC, Heng HHQ, Doyon-Reale N, Gregoire L, Lancaster WD, Rabah R, Schmelz EM. Sequential molecular and cellular events during neoplastic progression: A mouse syngeneic ovarian cancer model. Neoplasia. 2005; 7:944–956. [PubMed: 16242077]
24. Creekmore AL, Silkworth WT, Cimini D, Jensen RV, Roberts PC, Schmelz EM. Changes in Gene Expression and Cellular Architecture in an Ovarian Cancer Progression Model. PLOS ONE. 2011; 6:e17676. [PubMed: 21390237]
25. (a) Kedrin D, van Rheenen J, Hernandez L, Condeelis J, Segall JE. Cell motility and cytoskeletal regulation in invasion and metastasis. J Mammary Gland Biol Neoplasia. 2007; 12:143–152. [PubMed: 17557195] (b) Pawlak G, Helfman DM. Cytoskeletal changes in cell transformation and tumorigenesis. Curr Opin Genet Dev. 2001; 11:41–47. [PubMed: 11163149] (c) Provenzano PP, Keely PJ. Mechanical signaling through the cytoskeleton regulates cell proliferation by coordinated focal adhesion and Rho GTPase signaling. J Cell Sci. 2011; 124:1195–1205. [PubMed: 21444750]
26. Barkan D, Kleinman H, Simmons JL, Asmussen H, Kamaraju AK, Hoenorhoff MJ, Liu ZY, Costes SV, Cho EH, Lockett S, Khanna C, Chambers AF, Green JE. Inhibition of metastatic outgrowth from single dormant tumor cells by targeting the cytoskeleton. Cancer Research. 2008; 68:6241–50. [PubMed: 18676848]
27. (a) Gault CR, Obeid LM, Hannun YA. An overview of sphingolipid metabolism: from synthesis to breakdown. Adv Exp Med Biol. 2010; 688:1–23. [PubMed: 20919643] (b) Gangoiti P, Camacho L, Arana L, Ouro A, Granado MH, Brizuela L, Casas J, Fabriás G, Abad JL, Delgado A, Gómez-Muñoz A. Control of metabolism and signaling of simple bioactive sphingolipids: Implications in disease. Prog Lipid Res. 2010; 49:316–34. [PubMed: 20193711] (c) Ogretmen B, Hannun YA. Biologically active sphingolipids in cancer pathogenesis and treatment. Nat Rev Cancer. 2004; 4:604–616. [PubMed: 15286740]
28. Schmelz EM, Roberts PC, Kustin EM, Lemonnier LA, Sullards MC, Dillehay DL, Merrill AH Jr. Modulation of intracellular beta-catenin localization and intestinal tumorigenesis in vivo and in vitro by sphingolipids. Cancer Research. 2001; 61:6723–9. [PubMed: 11559543]
29. Teichgraber V, Ulrich M, Endlich N, Riethmuller J, Wilker B, De Oliveira-Munding CC, van Heeckeren AM, Barr ML, von Kurthy G, Schmid KW, Weller M, Tummler B, Lang F, Grassme H, Doring G, Gulbins E. Ceramide accumulation mediates inflammation, cell death and infection susceptibility in cystic fibrosis. Nat Med. 2008; 14:382–391. [PubMed: 18376404]
30. (a) Ryland LK, Fox TE, Liu X, Loughran TP, Kester M. Dysregulation of sphingolipid metabolism in cancer. Cancer Biol Ther. 2011; 11:138–49. [PubMed: 21209555] (b) Strub GM, Maceyka M, Hait NC, Milstien S, Spiegel S. Extracellular and intracellular actions of sphingosine-1-phosphate. Adv Exp Med Biol. 2010; 688:141–55. [PubMed: 20919652]
31. (a) Schmelz EM, Sullards MC, Dillehay DL, Merrill AH Jr. Colonic cell proliferation and aberrant crypt foci formation are inhibited by dairy glycosphingolipids in 1, 2-dimethylhydrazine-treated CF1 mice. J Nutr. 2000; 130:522–7. [PubMed: 10702579] (b) Lemonnier LA, Dillehay DL, Vespremi MJ, Abrams J, Brody E, Schmelz EM. Sphingomyelin in the suppression of colon tumors: prevention versus intervention. Arch Biochem Biophys. 2003; 419:129–38. [PubMed: 14592456] (c) Schmelz EM, Dillehay DL, Webb SK, Reiter A, Adams J, Merrill AH Jr. Sphingomyelin consumption suppresses aberrant colonic crypt foci and increases the proportion of adenomas versus adenocarcinomas in CF1 mice treated with 1,2-dimethylhydrazine: implications for dietary sphingolipids and colon carcinogenesis. Cancer Research. 1996; 56:4936–41. [PubMed: 8895747]
32. Simon KW, Tait L, Miller F, Cao C, Davy KP, Leroith T, Schmelz EM. Suppression of breast xenograft growth and progression in nude mice: implications for the use of orally administered

sphingolipids as chemopreventive agents against breast cancer. Food Funct. 2010; 1:90–8. [PubMed: 21776459]

33. (a) Hanna AN, Berthiaume LG, Kikuchi Y, Begg D, Bourgoin S, Brindley DN. Tumor necrosis factor-alpha induces stress fiber formation through ceramide production: role of sphingosine kinase. Mol Biol Cell. 2001; 12:3618–30. [PubMed: 11694593] (b) Singleton PA, Dudek SM, Chiang ET, Garcia JG. Regulation of sphingosine 1-phosphate-induced endothelial cytoskeletal rearrangement and barrier enhancement by S1P1 receptor, PI3 kinase, Tiam1/Rac1, and alpha-actinin. FASEB J. 2005; 19:1646–56. [PubMed: 16195373]
34. Li QS, Lee GYH, Ong CN, Lim CT. AFM indentation study of breast cancer cells. J Biochemical and Biophysical research communications. 2008; 374:609–613.
35. (a) Rico F, Roca-Cusachs P, Gavara N, Farre R, Rotger M, Navajas D. Probing mechanical properties of living cells by atomic force microscopy with blunted pyramidal cantilever tips. J Phys Rev E. 2005; 72:1–10.(b) Sen S, Subramanian S, Discher DE. Indentation and adhesive probing of a cell membrane with AFM: theoretical model and experiments. Biophysics J. 2005; 89:3203–3213.
36. Dimitriadis EK, Horkay F, Maresca J, Kachar B, Chadwick RS. Determination of Elastic Moduli of Thin Layers of Soft Material Using the Atomic Force Microscope. Biophysical J. 2002; 82:2798–2810.
37. Vinckier A, Semenza G. Measuring Elasticity of biological materials by atomic force microscopy. FEBS Letters. 1998; 430:12–16. [PubMed: 9678586]
38. Carl P, Schillers H. Elasticity measurement of living cells with an atomic force microscope: data acquisition and processing. Pflugers Arch. 2008; 457:551–559. [PubMed: 18481081]
39. Creekmore AL, Heffron CL, Brayfield BP, Roberts PC, Schmelz EM. Regulation of Cytoskeleton Organization by Sphingosine in a Mouse Cell Model of Progressive Ovarian Cancer. Biomolecules. 2013; 3:386–407.
40. Arce FT, Whitlock JL, Birukova AA, Birukov KG, Arnsdorf MF, Lal R, Garcia JGN, Dudek SM. Regulation of the Micromechanical Properties of Pulmonary Endothelium by S1P and Thrombin: Role of Cortactin. Biophysical J. 2008; 95:886–894.

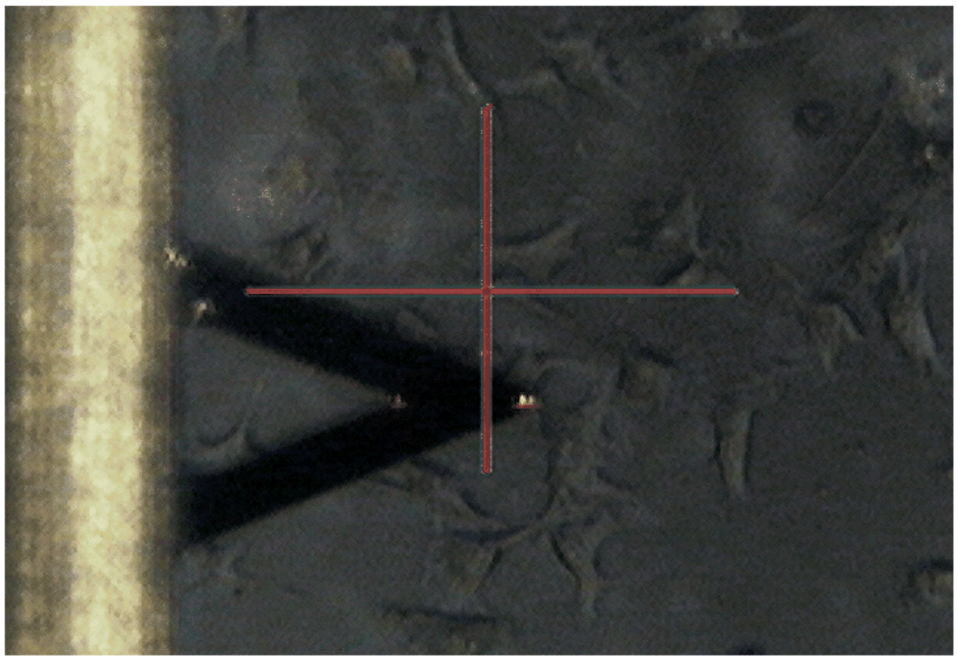

Fig. 1.
Actual screenshot of a V-shaped cantilever during indentation of randomly selected adherent single cells.

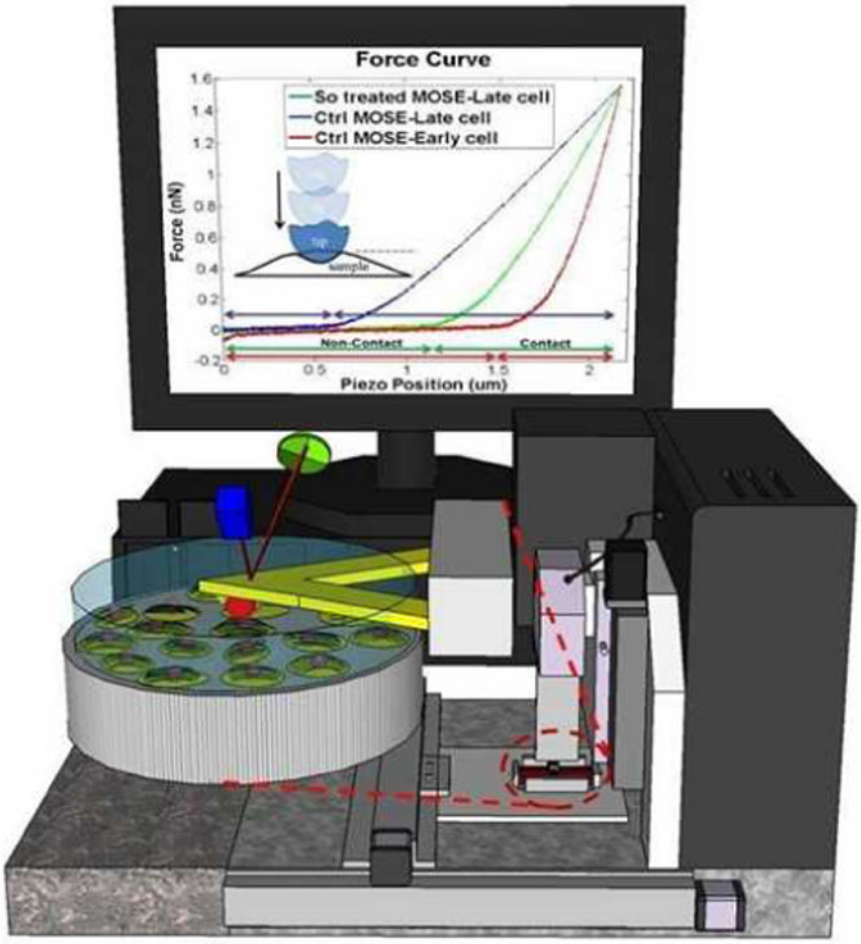

Fig. 2.

Schematic illustration of experiment setup. The monitor is showing force curves obtained via AFM indentations. Although the aggressive MOSE-L cell has lower slope reading compared to the healthier MOSE-E cell, its slope and consequently stiffness increases significantly after treatment with So.

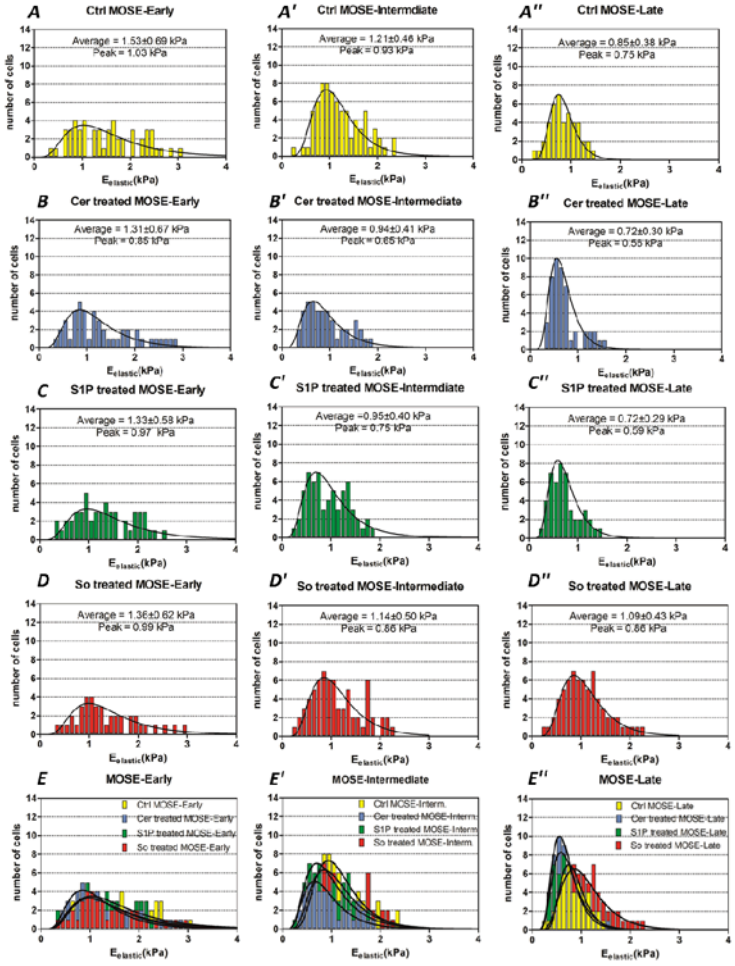

Fig. 3.

Histograms of MOSE-Late, MOSE-Intermediate, and MOSE-Early cells in control and Cer, S1P, and So treated conditions depict the changes in distribution of measured elastic modulus after treatments.

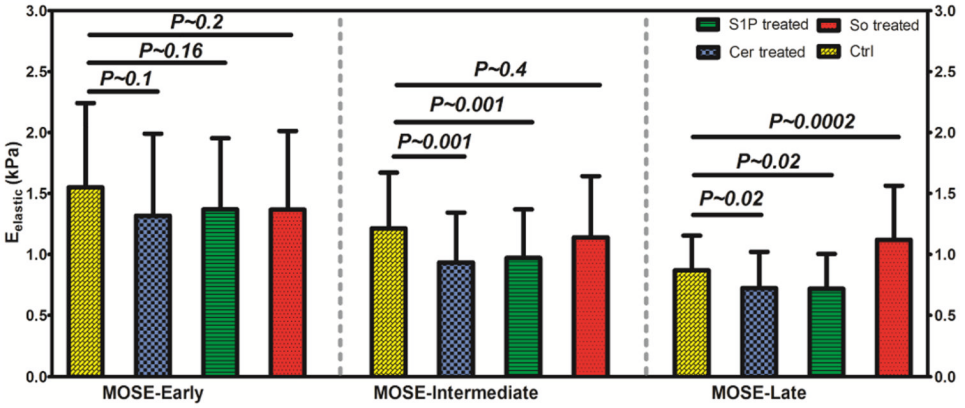

Fig. 4.

Depiction of changes in elastic modulus of early, intermediate, and late stage of MOSE cell lines as effects of treatment with So, Cer, and S1P in comparison to control counterparts.